International Journal of Food Microbiology 271 (2018) 24–32

Contents lists available at ScienceDirect

International Journal of Food Microbiology

journal homepage: www.elsevier.com/locate/ijfoodmicro

# Metabolite profiling of *Listeria innocua* for unravelling the inactivation mechanism of electrolysed water by nuclear magnetic resonance spectroscopy

Qin Liu[a,c], Ji'en Wu[b], Zhi Yang Lim[a], Shaojuan Lai[d], Norman Lee[e], Hongshun Yang[a,c,*]

[a] Food Science and Technology Programme, c/o Department of Chemistry, National University of Singapore, Singapore 117543, Singapore
[b] The Nuclear Magnetic Resonance Laboratory, Department of Chemistry, National University of Singapore, 3 Science Drive 3, Singapore 117543, Singapore
[c] National University of Singapore (Suzhou) Research Institute, 377 Lin Quan Street, Suzhou Industrial Park, Suzhou, Jiangsu 215123, PR China
[d] Guangzhou Pulu Medical Technology Co., Ltd, Guangzhou, Guangdong 510800, PR China
[e] Science Research Programme, Temasek Junior College, Singapore 469278, Singapore

ARTICLE INFO

*Keywords:*
*Listeria monocytogenes*
Sanitiser
Oxidative stress
NMR
Metabolomics

ABSTRACT

Bactericidal effects of low concentration electrolysed water (LcEW) on microorganisms are previously well reported; however, the inactivation mechanism of EW is not understood. The lethal and sublethal injuries of *L. monocytogenes* and *L. innocua* by EW treatments were determined and the metabolic profile changes for *L. innocua* were characterised using nuclear magnetic resonance (NMR). Microbial metabolomics approach combined with multivariate data analyses was used to interpret the cellular chemical fingerprints of *L. innocua*. The relative amount of intracellular reactive oxygen species (ROS) was assayed using 2′,7-dichlorodihydrofluorescein diacetate ($H_2$DCFDA). The results showed that the proportion of the sublethally injured microbial cells *L. monocytogenes* and *L. innocua* increased from 40% to 70% and from 35% to 65%, respectively, when the free available chlorine (FAC) of LcEW increased from 2 to 8 mg/L. Overall, 36 low-molecular-weight metabolic compounds in *L. innocua* extracts were characterised by NMR spectroscopy. EW perturbation resulted in a drastic and multitude disruption across a wide range of biochemical process including peptidoglycan synthesis, nucleotides biosynthesis and amino acid metabolism. Elevated levels of α-ketoglutarate and succinate implicated the enhanced glutamate decarboxylase (GAD) system and γ-aminobutyric acid (GABA) shunt for the protection against oxidative stress. These findings provided the comprehensive insights into the metabolic response of *Listeria* to EW oxidative stress and can serve as a basis for better utilisation for sanitisation.

## 1. Introduction

*Listeria monocytogenes* is pathogenic bacterial species responsible for severe infection, listeriosis (Morey et al., 2014). The high adaptation ability of *L. monocytogenes* and the different responses of *L. monocytogenes* to physicochemical interventions make its control in foods difficult (Ignatova et al., 2010). *L. innocua* is another species from the genus *Listeria*, and widely found in soil and ready-to-eat foods (Silva-Angulo et al., 2014). *L. innocua* is an innocuous and thus harmless to human health. *L. innocua* has been used as a nonpathogenic thermal processing surrogate for *L. monocytogenes*. The high similarity of serological, biochemical and morphological properties with *L. monocytogenes* and the fact that it is non-pathogenic makes *L. innocua* a great surrogate for studies (Friedly et al., 2008).

Low concentration electrolysed water (LcEW) has been increasingly used as a disinfectant in food decontamination due to its economic cost, low corrosivity and convenient quick on-site production (Zhang et al., 2016; Zhang et al., 2017; Zhao et al., 2017). The strong disinfection efficacy of LcEW against microorganisms has been demonstrated by many previous studies (Liu et al., 2017a; Sow et al., 2017; Yang et al., 2013; Zhang and Yang, 2017). The bactericidal effect of LcEW is partially due to its high oxidation potential (ORP) (940–1010 mV), which is outside the preferable redox potential range of most microorganisms (Park et al., 2004; Park et al., 2009). The high ORP is reported to generate oxidative damage to protein and DNA, resulting in the disturbance of the electron flow, and metabolic flux changes in cells (Huang et al., 2008). Liao et al. (2007) noted that the high ORP of EW may induce the formation of disulfide bridges, depletion of energy stores, and consequently disturbing metabolic pathways inside the cell. Liu et al. (2017b) found that nucleotides and amino acids in *Escherichia*

* Corresponding author.
*E-mail address:* chmynghs@nus.edu.sg (H. Yang).

https://doi.org/10.1016/j.ijfoodmicro.2018.02.014
Received 1 August 2017; Received in revised form 6 January 2018; Accepted 11 February 2018
Available online 14 February 2018
0168-1605/ 

*coli* were greatly affected by EW, indicating that metabolite profiles of bacteria can provide precise cellular responses resulting in EW-induced biochemical alterations.

Emerging metabolomic techniques have made it more feasible to acquire high-throughput profiles of bacteria metabolic status for enhancing the understanding of the mechanisms underlying oxidative stress and the resulting bacterial response. Some spectroscopic techniques, nuclear magnetic resonance (NMR) and gas chromatography–mass spectrometry (GC–MS), for instance, are increasingly used in the metabolic profile analysis of microbial extracts. In combination with multivariate analysis, NMR is able to give fast, informative, reproducible and stable metabolic profiling of microorganisms in time and require minimal sample preparation. Such metabolomic approaches have shown promising results in different fields including environmental stress, infrastructure biofilms, detection and differentiation of bacteria (Beale et al., 2014; Liu et al., 2017b; Ye et al., 2012a).

Although many studies showed that EW could efficiently kill pathogens, its impact on the global metabolic response of *Listeria* has not been completely elucidated yet. The objectives of present study were to examine metabolic profile changes and the affected pathways of *L. innocua* after LcEW treatment by NMR spectroscopy coupled with multivariate data analysis. *L. innocua* is commonly chosen as a good surrogate for *L. monocytogenes* in many preservation studies. It is of great interest to compare the inactivation and sublethal injury by EW treatments between the two microorganisms.

## 2. Methods and materials

### 2.1. Bacterial strains and their growth conditions

*L. monocytogenes* (smoked salmon isolate, serotype 3a) was kindly provided by Food Science and Technology Programme, National University of Singapore and stored at −80 °C. *L. innocua* ATCC® 33090™ was purchased from DSMZ (Deutsche Sammlungvon Mikroorganismen und Zellkulturen GmbH, Germany) and stored at −80 °C. Cells were resuscitated by inoculating into 10 mL Tryptone Soya Broth (TSB, Oxoid) and incubating at 37 °C for 24 h. A loopful of the suspension was then streaked onto Tryptone soya agar (TSA; Oxoid) and the plate was incubated at 37 °C for 24 h. To prepare cultures for experiments a loopful of a single colony was transferred into 10 mL TSB at 37 °C for overnight incubation (16–18 h). Cultures in exponential-phase were collected and processed by diluting the overnight culture 1:100 in fresh TSB and incubating at 37 °C until a final cell concentration of $10^8$ CFU/mL was reached. The optical density (OD) of the cultures was assayed at 600 nm to determine the cell concentration (CFU/mL) using a previously established relation between $OD_{600}$ and CFU/mL. Bacterial viable counts were determined by enumerating cells on TSA, using 0.1% (w/v) peptone water for decimal dilution.

### 2.2. Electrolysed water treatment and enumeration following treatment

EW was obtained from a model ROX-10WB Acidic EW generator (Hoshizaki Electric Company Ltd., Toyoake, Aichi, Japan) and the free chlorine level was measured using a reflectometer (Merck, Darmstadt, Germany). The EW used in this study had a pH range of 3.6–4.4, an oxidation reduction potential (ORP) of 910–1014 mV and 2–8 mg/L free available chlorine (FAC). In a preliminary study, several concentrations of EW with 0.5–32 mg/L FAC were tested to determine the maximum concentration that did not completely inhibit the growth of cells (data not shown). Based on the results obtained, 2–8 mg/L FAC levels for 5 min were selected for use in the sublethal injury test. The cells were washed twice with phosphate-buffered saline (PBS) buffer and re-suspended in PBS buffer. Subsequently, 9.5 mL of culture was added to treatment test tubes containing 0.5 mL EW (2, 4, 8 mg/L FAC final concentration). The samples with sterile distilled water (pH 6.5, FAC = 0 mg/L, ORP = 365 ± 14 mV) added at the same volume were considered as controls. Following treatment, treated cells were serially diluted in neutralising buffer (BD Biosciences) and spread onto non-selective medium TSA with 0.6% yeast extract (TSA-YE) and onto TSA-YE selective medium added with 5% sodium chloride (TSA-YE-SC). Colonies were enumerated after 48 h incubation at 37 °C. Colonies which appeared on TSA-YE were regarded as having developed from uninjured plus injured cells, while those which appeared on TSA-YE-SC were regarded as having developed by only uninjured cells. The experiments were conducted independently in triplicate. The extent of sublethal injured cells was expressed as the difference between the count (CFU) on nonselective medium (TSA-YE) and the count on selective medium (TSA-YE-SC). To determine the percentage of sublethally injured cells, following equation (Uyttendaele et al., 2008) was used:

$$[1 - (\text{count on TSA} - \text{YE} - \text{SC}/\text{count on TSA} - \text{YE})] * 100 \quad (1)$$

### 2.3. Detection and imaging of intracellular reactive oxidative species (ROS)

The oxidant-sensitive probe 2′,7-dichlorodihydrofluorescein diacetate ($H_2$DCFDA) was applied to assess the intracellular ROS generation levels in *L. innocua*. Briefly, bacteria were centrifuged, washed and resuspended in PBS buffer (pH 7.4). To measure the ROS species generated during treatment of bacteria with EW, *L. innocua* cells were pre-incubated with 200 μM final $H_2$DCFDA in the dark at 37 °C for 1 h. After the incubation with $H_2$DCFDA, the bacteria were washed and re-suspended in PBS. The suspension was then treated with EW for 5 min. Sodium thiosulfate of 0.5% was added to quench the excess FAC. The bacteria were pelleted, washed, resuspended in the buffer and disrupted by sonication. For all sanitation treatments, 100 μL of the *L. innocua* suspension were transferred into each well of a 96-well plate (Corning, Tewksbury, MA, USA). The fluorescence intensity was recorded by a fluorescence plate reader (Spectrafluor Plus, Tecan, Durham, NC, USA), with excitation/emission wavelengths of 488/520 nm. The pre-incubated *L. innocua* were examined under confocal fluorescent (excitation: 485 nm, emission: 535 nm) microscope (Olympus FV1000, Japan) (Marcén et al., 2017). All conditions were tested in triplicate.

### 2.4. Extraction of intracellular metabolites

Overnight-grown cultures (1 mL) were washed and diluted to 1:100 (v/v) in a freshly prepared TSB and cultivated at 37 °C until a final cell concentration of $10^8$ CFU/mL was reached. Following this, cells were either added with distilled water (control) or stressed by adding EW at 4 mg/L FAC with a short vortex duration. After 5 min of treatment, the cell cultures were quenched with a brief incubation on ice, followed by centrifugation (5000 *g*, 5 min, 4 °C), the supernatant was decanted and discarded (Bhattacharyya et al., 2016). The chilling method avoided introducing other solvents to the extraction system. The cell pellets were washed six times with ice-cold PBS (pH 7.4) to remove the glucose and other components from the TSB and thus all metabolites detected were coming from the *Listeria* cell and not from the medium. Cell pellets were then resuspended in 600 μL extraction solution and sonicated (80 kHz, 100 W) on wet ice for 25 cycles with each cycle with 5 s pulse and 10 s stops. Extraction solution was prepared by mixing equal volumes of $NaH_2PO_4$-$K_2HPO_4$ buffer (0.1 mol/L, pH 7.4, containing 10% $D_2O$ and acetonitrile (Liu et al., 2017b; Ye et al., 2012a). The metabolites from lysed cells were obtained by centrifugation at 5000 *g* at 4 °C for 10 min. The remaining solid residues were extracted further with the same quantity of extract solution and homogenised by vortex. The secondary supernatant was obtained after centrifugation and pooled with the first extraction. Acetonitrile was then removed from pooled supernatant by rotary evaporator. For each sampling point, 5 replicate samples were prepared. The samples were then stored at −80 °C for NMR and GC/MS analyses (Ye et al., 2012b).

### 2.5. NMR acquisition

For NMR analysis, after solvent removal of acetonitrile, 550 μL of the extract in phosphate buffer containing 10% $D_2O$ was transferred into a 5-mm NMR tube. All NMR measurements were performed at 298 K using a Bruker DRX-500 NMR Spectrometer via a Triple Inverse Gradient (TXI) probe (Bruker, Germany). For each sample, the $^1H$ NMR spectra were obtained using a first increment of NOESY pulse sequence (recycle delay-90°-$t_1$-90°-$t_m$-90°-acquisition). Water suppression was obtained by a weak continuous wave irradiation during both the recycle delay (RD, 2 s) and the mixing time ($t_m$, 100 ms). The $t_1$ was set as 6.5 μs and the 90° pulse length was modified to around 10 μs. For each spectrum, sixty-four induction decays were collected into 32 k data points with a spectral width of 17 ppm. All free induction decays (FIDs) were multiplied by an exponential function equivalent to a 1-Hz line-broadening factor prior Fourier Transformation (FT) (Ye et al., 2012b).

### 2.6. Gas chromatography/mass spectrometry (GC/MS)

For GC/MS analysis, 600 μL of the collected extract was lyophilised, resuspended in 200 μL of pyridine containing methoxyamine HCl (20 mg/mL), and incubated at 40 °C for 90 min. The mixtures were then treated with 100 μL of *N*-Methyl-*N*-(trimethylsilyl)trifluoroacetamide (MSTFA) at 50 °C for 30 min. Metabolites were injected in a 1:10 split mode at 260 °C, a helium column flow of 119 mL/min was used. The column was prepared at 70 °C for 5 min via a temperature gradient of 5 °C/min to a final temperature of 360 °C, with a 2 min holding time.

### 2.7. Spectral processing and statistical analysis

The resulting NMR spectra from control and EW treated samples were phased and baseline corrected manually with TopSpin 4.2 (Bruker Biospin, Rheinstetten, Germany)/Chenomx NMR Suite 8.1 (Chenomx Inc., Edmonton, Canada). Data reduction was accomplished by dividing the spectrum from δ 8.5 to 0.5 into regions bucket with width of 0.02 ppm using Mnova (Mestreab Research SL, Santiago de Compostela, Spain). The solvents signals (water and acetonitrile) were excluded and the standardised binned data was used for multivariate data analysis. The spectral dataset was then constructed and imported into a SIMCA-$P^+$ software (version 13.0, Umetrics, Sweden) for multivariate analysis. Data sets were subject to principal components analysis (PCA) and orthogonal partial least squares discriminant analysis (OPLS-DA), an extension of the supervised partial least squares regression (PLS regression) method in order to enhance the quality of the classification model (Jadhav et al., 2015). OPLS-DA facilitates model interpretation by separating the systematic variation in X into two parts: linearly related to Y and orthogonal to Y, respectively (Wiklund et al., 2008). Loading and coefficient plots were analysed to indicate the variables that has class discriminating power in order to detect the metabolites that affect the group membership (colour coding visualisation). Moreover, variable importance in projection (VIP) was performed on the preprocessed spectra using the algorithms included in the OPLS-toolbox. This was to reveal the metabolites primarily influencing the samples' differentiation. For instance, terms with a VIP value > 1 influenced mostly the extracted OPLS models (Fotakis and Zervou, 2016). Metabolic pathways analysis was performed by MBrole (http://csbg.cnb.csic.es/mbrole2/) to recognise the affected metabolic pathways and contribute to further biological interpretation (Chagoyen and Pazos, 2011). MBRole allows categorisation of metabolite compounds according to their biological annotation (enrichment analysis) in metabolomics database.

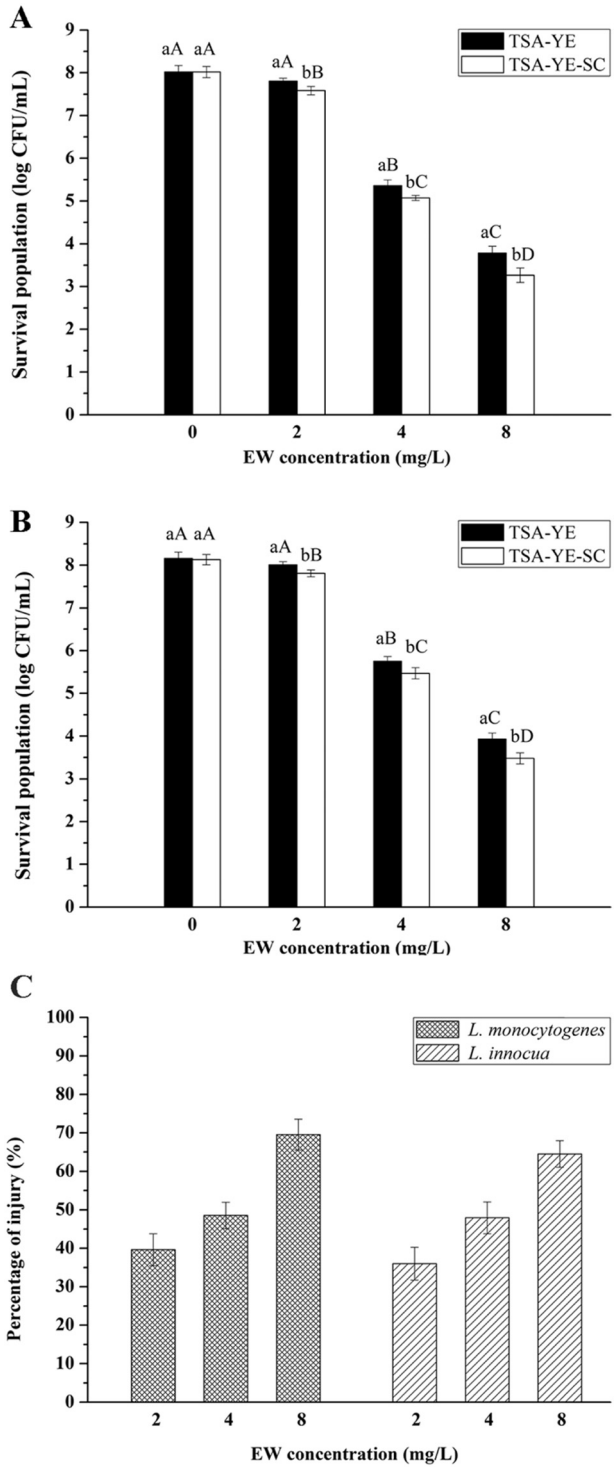


**Fig. 1.** Surviving of *L. monocytogenes* (A) and *L. innocua* (B) and sublethally injured percentage (C) of cells treated by electrolysed water (EW) at different concentrations ($n$ = 3). Data are presented as means ± standard deviation. Means within same concentration with different small case letters are significantly different; means for same medium at different concentrations with different capital letters are significantly different.

## 3. Results and discussion

### 3.1. Survival of L. monocytogenes and L. innocua after EW treatments

The inactivation of *L. monocytogenes and L. innocua* after EW treatment at 2, 4, 8 mg/L FAC for 5 min were studied by counting survivors

on the nonselective (TSA-YE) and selective (TSA-YE-SC) media. Fig. 1 shows that *L. monocytogenes* and *L. innocua* exhibited similar trends of decreased survival population with increased EW treatment. The initial population of *L. monocytogenes* and *L. innocua* were approximately 8.0 ± 0.2 and 8.2 ± 0.2 log CFU/mL, respectively. No significant differences ($P > 0.05$) of the TSA-YE survival populations were found among control and the 2 mg/L FAC group of both *L. monocytogenes* and *L. innocua*. However, the number of both TSA-YE and TSA-YE-SC survival cells in 4 mg/L treated group was significantly less than numbers in control group ($P < 0.05$) of both *L. monocytogenes* and *L. innocua*. Populations measured on TSA-YE-SC of both *L. monocytogenes* and *L. innocua* were consistently lower than those on TSA-YE by approximately the same 0.2–0.5 log CFU/mL indicating that cell injury had occurred and that injury was more pronounced at higher EW concentration.

As shown in Fig. 1c, when bacterial cells were treated with EW, the proportion of sublethally injured cells increased with increasing EW doses; the one-way ANOVA indicated significant differences between EW levels ($P < 0.05$) for both *Listeria* species. Regarding the sublethal percentage of *Listeria* species caused by exposure to EW, sublethally injured percentage of *L. monocytogenes* and *L. innocua* ranged from 40% to 70% and from 35% to 65%, respectively. The highest proportion of injured cells was found when the cells were treated with EW at 8 mg/L FAC. These results are consistent with those obtained by Xuan et al. (2017) for *L. monocytogenes*. The study showed that a 40-s treatment with EW (FAC = 7.5 mg/L) led to a reduction of *L. monocytogenes* by 3.5 log CFU/mL and sublethally injured rate of 80%. Microbial inactivation by EW is thought to be generated by the perturbation and effects of EW on redox couple, membrane transport capacity and functionality, DNA synthesis and enzyme activity essential for bacteria growth (Liao et al., 2007; Rahman et al., 2016).

*L. innocua* was widely proposed as a good surrogate for *L. monocytogenes* in a variety of disinfection technologies. In this study, the pathogenic and nonpathogenic strains showed nearly equal resistance to EW treatment and exhibited similar sublethal injury at 2–8 mg/L FAC levels. Therefore, these identical findings suggest that *L. innocua* ATCC 33090 has the potential for use as a surrogate in EW treatments.

Microorganisms that survive a given stress often have increased resistance to antibiotics and altered virulence characteristics via cross-protection. Therefore, the occurrence of sublethally injured cells in foods may pose public health concerns and is critical assessing the microbial response to food preservation treatments. Sub-lethal injury usually relates to stress adaptation of microorganisms and the injury could be either structural or metabolic. Usually, metabolic injury is due to damage to various functional components of the cells and antibiotic resistance in bacteria is often associated with a metabolic burden (Wesche et al., 2009). On the basis of the current results in which sublethally damaged cells after exposure to EW were observed, the study of metabolic changes in *L. innocua* treated with EW were proceeded at the sublethal concentration.

### 3.2. Measurement of intracellular reactive oxidative species (ROS) and protein leakage of bacteria suspension

The fluorescence intensity was measured for the control *L. innocua* sample as well as for the sample treated with EW (FAC = 1, 2, 4 and 8 mg/L). The increased fluorescence intensity indicated the activation of the fluorescent dye probe by peroxide molecules and hydroxyl radicals. The samples treated with EW showed a significant higher intensity as compared to the control, indicating generation of intracellular ROS in *L. innocua* immediately upon EW exposure (Fig. 2A). As shown in Fig. 2B, number of fluorescent *L. innocua* labelled with $H_2$DCFDA increased with an increase in EW concentration, compared to the control cells. Correlation analysis between fluorescence signals and log reduction of bacteria cells showed a strong correlation ($P < 0.05$) with Pearson Correlation Coefficient (PCC) value of 0.93, indicating the significant relationship between the survival count reduction and fluorescence intensity changes from $H_2$DCFDA labelled cells. Jeong et al. (2006) demonstrated that ROS as the additional disinfectants, such as $O_3$ and ·OH generated by EW, can contribute a lot in microorganism inactivation, as much as chlorine component in the electrochemical disinfection. The changes of bacteria induced by EW were viewed as similar to that caused by the ·OH formed from Fenton reaction (Diao et al., 2004).

The changes of protein leakage of *L. innocua* as the treatment with EW proceeded are shown in Fig. 2C. The leakage of protein after EW treatments at 1, 2, 4 and 8 mg/L significant increased due to the damage on the cell outer membrane. However, the results were unexpected as the protein leakage did not show any trend when subject to different EW concentrations. Correlation analyses assured the absence of correlation between the protein leakage and the logarithmic reduction of the bacterial count (Fig. 2D). The leakage of cytoplasmic proteins indicated the damage of the cell's outer permeability barriers and the marked conformational changes in cell membrane. The results in this study indicated that EW could induce significant effects on functionality of outer membrane. However, this damage may not be the leading mechanisms of low concentration EW for bactericidal activity since the correlation analyses suggested no correlation between the fluorescence intensity and the log reduction in bacterial survival of *L. innocua*. Possible antimicrobial mechanism of EW may be due to potential oxidative damage to intracellular enzyme and perturbations of metabolite levels (Rahman et al., 2016).

### 3.3. $^1$H NMR metabolic profile

The resonances signals were assigned to individual metabolites with $^1$H data according to previous investigations (Ye et al., 2012a, b) and confirmed by comparing the resonance to the Chenomx NMR Suite, Human Metabolome Database (HMDB) and Biological Magnetic Resonance Data Bank (BMRB). The typical NMR spectrum of *L. innocua* extracts from control group is shown in Fig. S1. Full width $^1$H NMR spectra of the control and EW treated *L. innocua* are shown in supplemental Fig. S2. A visual inspection of these spectra revealed differences. The corresponding resonances were in good agreement with the database standard assignment. To the best of our knowledge, this was the first comprehensive report of the low-molecular-weight metabolites in *L. innocua* upon electrolysed water treatment. Thirty-eight metabolites were detected in extract samples, including organic acids, amino acids, nucleic acids. The peaks observed were due to the chemical shifts arising from protons being in different positions of the molecules, and the chemical shifts ranged from roughly 0 to 10 ppm, and was dependent on the nature of other adjacent protons atoms and the functional groups on the protons atoms. Since each detectable metabolite usually contains more than one resolvable resonance signal, if one overlapping spot cannot be identified, it is possible that the $^1$H chemical shift signals comprised in other regions coming from the same metabolites with equivalent signals in the spectrum.

The NMR typical spectrum of *L. innocua* extract reveals a preponderance of signals linked to amino acids like leucine, valine, alanine, lysine and aspartate, between 0.5 and 4.5 ppm. Some metabolites involved in citric acid cycle were present as well (acetate, 2-oxoglutarate, and succinate). In the region between 5.0 and 9.0 ppm, aromatic compounds such as adenosine 2′-3′-cyclic phosphate (2′,3′-cAMP), as well as ribose-5-phosphate, fumarate, and nicotinate, and nucleotides like AMP and UMP. The key identified metabolites are summarised in Table 1.

### 3.4. Alteration of metabolites upon EW treatment on L. innocua

Metabolic profiles of *L. innocua* extracts, obtained by $^1$H NMR spectroscopy, were therefore analysed with multivariate analyses (PCA, OPLS-DA) conducted on bucket reduced NMR spectra. The bucket

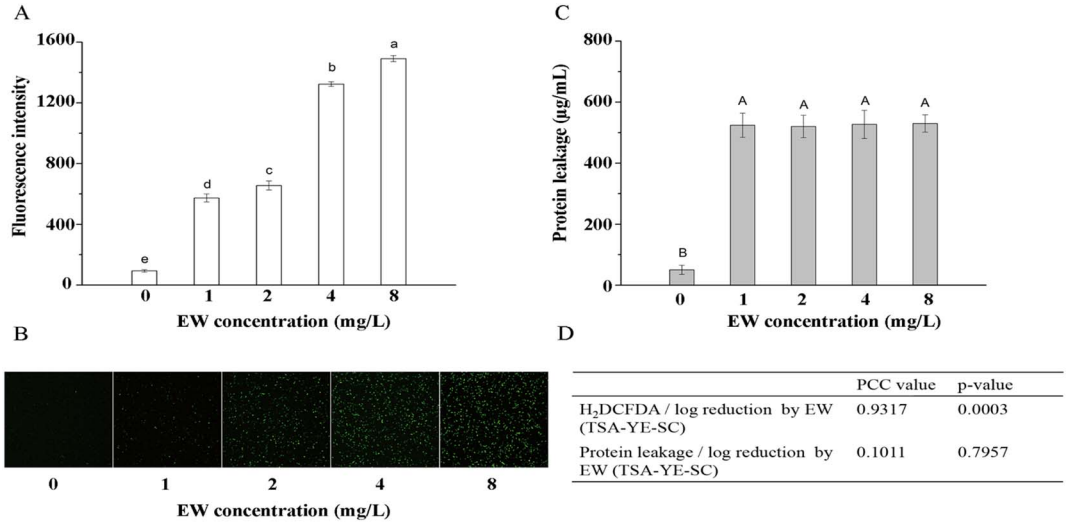


**Fig. 2.** Effect of electrolysed water on intracellular ROS accumulation and protein leakage in *L. innocua*. (A) Oxidative stress in *L. innocua* upon treatment with EW was measured by $H_2$DCFDA; (B) Representative confocal images of cells from different treatments stained with $H_2$DCFDA probe; (C) Protein amounts released into the cell suspension from electrolysed water (EW) treated *L. innocua* cells; (D) The Pearson correlation coefficient (PCC) between the logarithmic reduction, protein leakage and the $H_2$DCFDA fluorescence intensity. ($n$ = 3).

**Table 1**
Chemical shifts assignment, multiplicities and some coupling constants (*J*) of metabolites present in *L. innocua* extract.

| No. | Metabolic compounds | Chemical shifts (ppm) and multiplicity (*J* in Hz) |
|---|---|---|
| 1 | 2-Hydroxyisovalerate | 0.8 (d), 2.0 (m), 3.8 (d) |
| 2 | Valine | 0.9 (d, 6.9 Hz) |
| 3 | β-Hydroxybutyrate | 1.20 (d, 6.26 Hz) |
| 4 | *N*-Acetyl alanine | 1.33 (d, 7.28 Hz) |
| 5 | Lactate | 1.49 (d) |
| 6 | Alanine | 1.59 (d, 7.3 Hz) |
| 7 | Leucine | 1.72 (t) |
| 8 | Putrescine | 1.78 (m) |
| 9 | Lysine | 1.87 (t), 3.03 (t, 7.5 Hz) |
| 10 | Acetate | 1.92 (s) |
| 11 | Acetamide | 2.01(s) |
| 12 | Methionine | 2.21 (m) |
| 13 | 2-Oxoglutarate | 2.40 (d), 2.08 (d) |
| 14 | Succinate | 2.41 (s) |
| 15 | Aspartate | 2.52 (dd, 8.8, 17.5 Hz) |
| 16 | Methylamine | 2.57 (s) |
| 17 | Dimethylamine | 2.61 (s) |
| 18 | Malate | 2.68 (d) |
| 19 | Trimethylamine | 2.90 (s) |
| 20 | Choline | 3.21(s) |
| 21 | o-Phosphocholine | 3.22 (s) |
| 22 | Betaine | 3.29 (s), 3.89 (s) |
| 23 | Glycine | 3.56 (s) |
| 24 | Ribose-5-phosphate | 5.48 (m) |
| 25 | Uridine | 5.93 (d) 5.79 (d), 7.42 (d) |
| 26 | Cytidine | 5.79 (d), 6.01 (d, 6.9 Hz) |
| 27 | Fumarate | 6.38 (s) |
| 28 | Tyrosine | 6.90 (d) |
| 29 | Phenylalanine | 7.28 (m) |
| 30 | Uracil | 7.40 (d, 7.6 Hz) |
| 31 | Xanthine | 7.91 (s) |
| 32 | UMP | 8.06 (d) |
| 33 | Oxypurinol | 8.21 (s) |
| 34 | AMP | 8.23 (s) |
| 35 | Adenosine 2′-3′-cyclic phosphate | 8.37 (s) |
| 36 | Nicotinate | 8.47(d, 5.4 Hz) |

Multiplicity: s-singlet, d-doublet, t-triplet, q-quartet, m-multiplet.

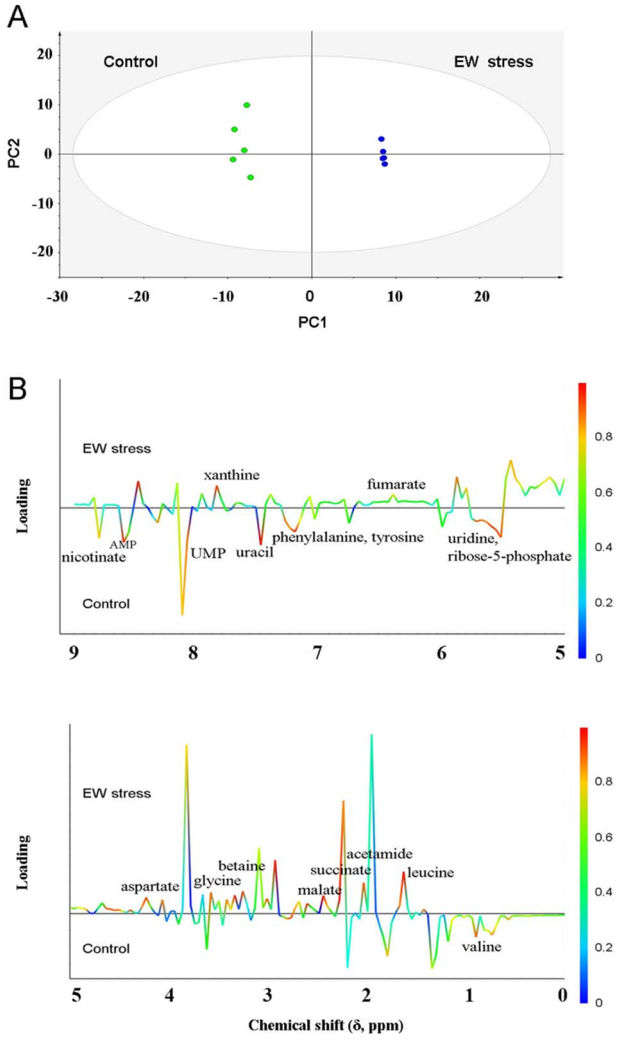


**Fig. 3.** PCA score plot (A) and coefficient-coded loading plots (B) by OPLS-DA analysis derived from NMR data of *L. innocua* for electrolysed water (EW) stress and control group. The lower sections in OPLS loading plot represent the metabolites that were higher in the control group compared to those from EW stress group.

reduced NMR spectra dataset was then constructed for the following multivariate data analysis. Initially, PCA analysis was performed to generate an overview of the metabolic alterations, which was accomplished using the score plot (Fig. 3A). The PCA analysis of the

normalised NMR data from bacterial extract samples was constructed based on the first two principal components (PC1 and PC2) for evaluating the metabolic alteration induced by EW stress. First two components explained 74.3% of total variance indicating the metabolites distribution in the space. The visual inspection of score plot showed a clear and strong separation for the *L. innocua* extract samples along PC1 component ($R^2$ (X) = 0.973, $Q^2$ = 0.819).

For further revealing the metabolites compounds responsible for the class separation, supervised data analysis tool OPLS-DA was applied with the corresponding NMR data via the pair-wise cell groups. The NMR spectra data was scaled to unit variance to reveal the effects of EW stress on the metabolic profiles (van den Berg et al., 2006; Ye et al., 2012b). The values for $R^2$ and $Q^2$ were employed as initial indicators for evaluating the goodness of fit (percentage variation explained by the model) and the predictability (fraction of the total variation of the Xs that is predictable) of the models generated by the analyses. Metabonomic analyses of *L. innocua* NMR spectra revealed strong separation and high predictability ($R^2$ (Y) = 0.997, $Q^2$ = 0.855) of the OPLS-DA model.

Incorporated colour-coded correlation coefficient based on chemical shifts is shown in Fig. 3B. The coefficient loading plot was drawn by extracting statistically and potentially significant metabolites in biochemical pathways, from their contributions to the model reliability (Wiklund et al., 2008). Peaks which pointed upwards showed higher amounts of specific metabolites detected from the EW stressed group, while peaks which pointed downwards had metabolites found in higher concentrations in the control group. Correlation coefficient values illustrated the weights of the discriminatory variables in terms of their strength to discriminate the classes. Specifically, as the colour of the peak gradually changes from cool colours (i.e. blue) to hot colours (i.e. red), the absolute value of the correlation coefficient increases from 0 to 1, indicating the resonances important for discriminating the metabolite profiles of pairwise control and EW stressed group (Liu et al., 2017b). The dominant metabolites (with significant correlation) that differed between concentrations are displayed in OPLS-DA coefficient plots.

The coefficient plot shows the increase or decrease in concentration of the metabolites identified. The analysis shows that control and EW stressed *L. innocua* are different at the biochemical level. Compared with the control, *L. innocua* treated with 4 mg/L FAC EW induced elevated levels of xanthine, fumarate, aspartate, glycine, betaine, malate, succinate, acetamide, leucine and decreases level of AMP, UMP, nicotinate, uracil, phenylalanine, tyrosine, uridine, ribose-5-phosphate, valine, highlighting the general changes in the metabolic network caused by EW. According to coefficient loading plots, chemical shift bins of 0.8–3.5 ppm displayed the most altered compounds, and these can mostly be assigned to organic acid and amino acids. In the presence of EW, a number of free radical systems are capable of catalysing the oxidative modification of functional molecules (Mahmoud et al., 2006). Among biological molecules, small peptide bonds (amide bond), amino groups, and thiol groups have high susceptibility to oxidative stress (Nightingale et al., 2000). Amino acids contain various reactive residues, making them potentially useful markers for oxidative stress. Free radicals are predicted to react with amino groups (e.g. histidine, lysine residues) to yield chloramines and further decomposed to protein-derived nitrogen-centred radicals via N—Cl bonds, which are the key species involved in the DNA oxidation and proteins fragmentation (Hawkins et al., 2002).

In order to identify the vital metabolites that were significant for EW-elicited effects to discriminate classes, VIP scores were calculated and assigned to metabolite variable as a composite indicator of a metabolite's importance to the model from the overall contribution to $R^2$ and $Q^2$ (Liu et al., 2017b). The absolute value, VIP = 1, was applied as the cutoff point for statistical significance based on the discrimination significance. Variables with a VIP score > 1 implied a significant contribution of metabolite intensity to the multivariate model and could be considered important in a given model (Fotakis and Zervou, 2016).

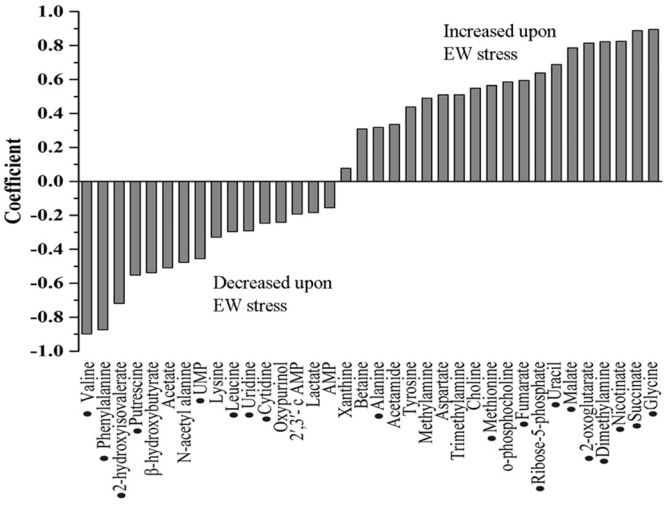


**Fig. 4.** The OPLS coefficient plots comparing the metabolic profile of electrolysed water (EW) treated and control *L. innocua*. The black dots indicate which metabolites contribute significantly to the OPLS-DA models (VIP > 1, see Materials and Methods for further details). $R^2$ X = 0.765, $Q^2$ Y = 0.855.

The metabolite concentration alteration of control and stressed were compared using OPLS-DA and the coefficient plot is shown in Fig. 4. The compounds with $VIP_{score} > 1$ and $P < 0.05$ for comparison of control and treated group were considered as statistically significant for discrimination of two classes, and thus possibly biochemically connected metabolites for the characterisation of the EW response to *L. innocua*. The analyses showed that control and EW stressed *L. innocua* were different at biochemical level, with valine and glycine causing the most difference between the classes. The results here revealed that the variations of several metabolites such as valine, leucine, uridine, cytidine, alanine, methylamine, fumarate, ribose-5-phosphate, uracil, malate, 2-oxoglutarate, succinate, glycine upon addition of EW were important in discriminating EW treated *L. innocua* from the control in the OPLS-DA model. The concentration variation of some important metabolites including fumate, malate, α-ketoglutamate, alanine, proline, lysine, valine was determined by GC/MS. Fig. 5 shows the difference in concentrations of certain specific metabolites found in both the control and the EW treated samples.

Fumarate and malate are organic acids which are critical

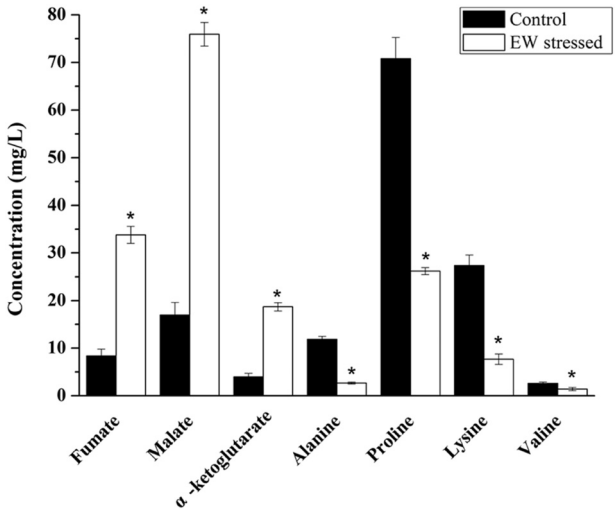


**Fig. 5.** Comparison of metabolite concentrations in *L. innocua* determined by GC/MS. *$P < 0.05$ (Student's *t*-test).

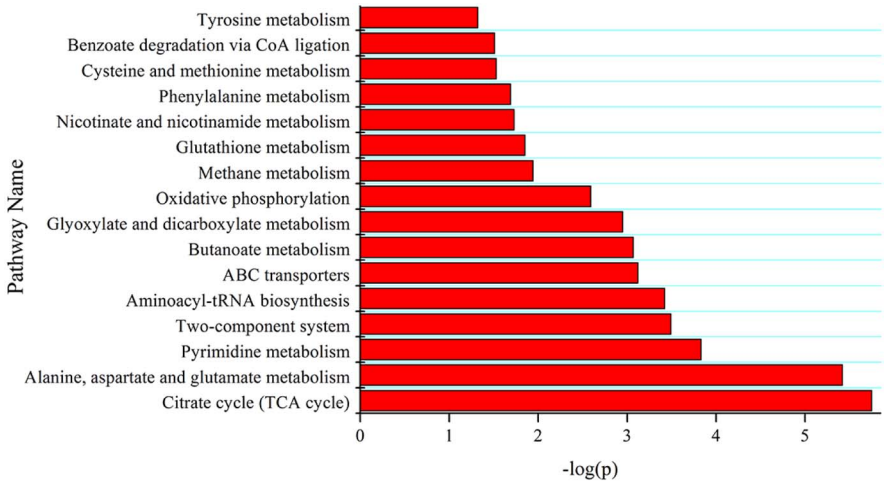


**Fig. 6.** Summary plot for metabolite set enrichment analysis of metabolic response to electrolysed water (EW) stress by using MBrole.

metabolites in the TCA cycle. After EW treatment, their concentrations increased drastically, implying the elevated rate of TCA flux. Ketoglutarate is a precursor of gamma-aminobutyric acid (GABA), which is an important metabolite used to resist oxidative stress (Bearson et al., 2009). The increased production of α-ketoglutarate implied that the microorganism took the advantage of GABA metabolism in response against EW stress (Feehily and Karatzas, 2013).

### 3.5. Metabolic pathway analysis

To identify the most relevant pathways that are most probability to be linked to the EW response, metabolic pathway analysis was performed according to the metabolite involvement in pathways that combined functional enrichment analysis and network analysis (Huang et al., 2009). In this study, MBrole (Chagoyen and Pazos, 2011) was used to explore the affected metabolic pathways, each providing virtually identical values. Only the metabolites with a $VIP_{score} > 1$ were submitted to MBrole analysis. Pathways with a false discovery rate $P < 0.05$ were thought as affected by EW stress exposure.

As shown in Fig. 6, sixteen pathways were suggested to be associated with the response to EW ($P < 0.05$). These pathways included citrate cycle (TCA cycle), pyrimidine metabolism, alanine, aspartate and glutamate metabolism, aminoacyl-tRNA biosynthesis, glyoxylate and dicarboxylate metabolism, etc. A complete list of pathway analysis results can be found in Fig. 6. Furthermore, KEGG database was used to link and integrate the metabolic pathways, which clearly clarified the perturbation upon EW stress treatment.

The main pathways of *L. innocua* metabolism affected by EW stress are summarised and sketched in Fig. 7. The figure indicated that EW stress perturbed the metabolic status of *L. innocua* involving many related metabolic pathways. Metabolites coloured in green refers to an increased concentration of metabolites in EW-treated cells while metabolites in red refers to a decreased concentration.

A balance between ROS generation and ROS destruction system is critical for maintaining cellular function. The excessive amount of ROS inside cells results in oxidative stress, loss of cell function, and necrosis or apoptosis. Peptidoglycan confers significant mechanical strength to Gram-positive bacteria and is known to be composed of linear peptidoglycan strands cross-linked *N*-acetylmuramic acid. In the EW treated group, the deceased level of alanine and lysine inhibited the cell proliferation since alanine and lysine are muramyl pentapeptide precursors that required for peptidoglycan biosynthesis (Liu et al., 2017b; Ye et al., 2012a). With alanine and lysine metabolism affected, the regeneration cell walls of *L. innocua* could be an obstacle to EW-treated samples. The depleted levels of amino acids such as valine, lysine, phenylalanine following EW treatment was in agreement with amino acid biosynthesis being very sensitive to oxidation (Jozefczuk et al., 2010). Amino acids are major osmoregulation solutes, which are capable of maintaining the normal osmolality of the cytoplasm and preventing the collapse of subcellular structures. The decrease level of several amino acids implied the osmotic alteration caused by EW (O'Byrne and Booth, 2002).

After sublethal injury, many microorganisms have manifested increased resistance to environmental stress and microbial control strategies, and maintained or enhanced their virulence. For example, in response to oxidative stress, microorganisms may react rapidly to attempt to repair the damage caused, using, for example, the glutamate decarboxylase (GAD) system and γ-aminobutyric acid (GABA) shunt (Bearson et al., 2009; Coleman et al., 2001). GAD system is one of the principle systems utilised by bacteria to cope with oxidative stress, a reaction that yields γ-aminobutyric acid (GABA) from glutamate. The GABA shunt, a pathway that metabolises GABA to succinate, presenting a possible compensatory pathway to partially overcome the incomplete TCA cycle of *Listeria*, which has been demonstrated that this pathway plays a critical role in the survival of bacteria under acidic and oxidative stress (Coleman et al., 2001). Previous studies have suggested that GABA shunt-related metabolites (GABA, glutamate) attempt to accumulate in response to oxidative stress (AL-Quraan, 2015). In this current report, a marked elevation of α-ketoglutarate and succinate was observed in EW treated *L. innocua*. Based on these findings, it is likely that the increased levels of α-ketoglutarate are used for synthesis of GABA during EW stress.

The pentose phosphate pathway was also found affected by EW-induced oxidative stress. The particular highlight was the depleted level of ribose-5-phosphate, which was a vital precursor for the synthesis of nucleotides. The uridine and cytidine was diminished correspondingly and therefore in turn led to the decrease of DNA and RNA biosynthesis. Such effects of decrease in nucleotide biosynthesis were direct indicators of DNA replication, cell division and growth status, revealing a pronounced adverse effect on cell proliferation (Bhat et al., 2015).

## 4. Conclusion

The present study shows that informative data obtained by NMR on the cellular metabolites may serve as an efficient method to identify the EW induced stress effect. The oxidative stress of EW produced a panel of metabolites response involving the alteration of organic acids, amino acids, nucleotide bases. Such changes led to a series of primary pathway alteration with reduced cell division as a possible mechanism of bactericidal action of EW. This study was an example of how microbial metabonomics approach combined with multivariate data analysis might contribute the knowledge of understanding low electrolysed water and low strength sanitisation treatment in food matrix. However,

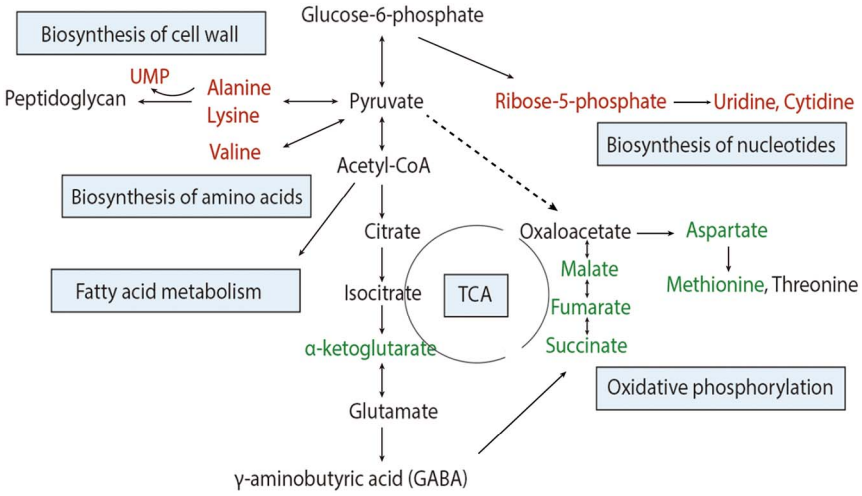


**Fig. 7.** Overview of metabolic alterations upon electrolysed water (EW) treatment. Metabolites depicted in green and red represent a higher and lower levels respectively in EW stressed *L. innocua* compared with the controls. (For interpretation of the references to colour in this figure legend, the reader is referred to the web version of this article.)

more in-depth investigations are necessary for revealing the specific molecular targets response for better understanding the associated bactericidal mechanism on bacteria communities.

Supplementary data to this article can be found online at https://doi.org/10.1016/j.ijfoodmicro.2018.02.014.

## Acknowledgements

We acknowledge the financial support by projects 31371851 and 31071617 supported by NSFC, Applied Basic Research Project (Agricultural) Suzhou Science and Technology Planning Programme (SYN201522), Singapore Ministry of Education Academic Research Fund Tier 1 (R-143-000-583-112), and an industry project supported by Guangzhou Kaijie Power Supply Industry Co., Ltd. (R-143-000-576-597).

## References

AL-Quraan, N.A., 2015. GABA shunt deficiencies and accumulation of reactive oxygen species under UV treatments: insight from *Arabidopsis thaliana* calmodulin mutants. Acta Physiol. Plant. 37, 1–11.

Beale, D.J., Morrison, P.D., Palombo, E.A., 2014. Detection of *Listeria* in milk using non-targeted metabolic profiling of *Listeria monocytogenes*: a proof-of-concept application. Food Control 42, 343–346.

Bearson, B.L., Lee, I.S., Casey, T.A., 2009. *Escherichia coli* O157: H7 glutamate-and arginine-dependent acid-resistance systems protect against oxidative stress during extreme acid challenge. Microbiology 155, 805–812.

Bhat, S.V., Booth, S.C., Vantomme, E.A., Afroj, S., Yost, C.K., Dahms, T.E., 2015. Oxidative stress and metabolic perturbations in *Escherichia coli* exposed to sublethal levels of 2, 4-dichlorophenoxyacetic acid. Chemosphere 135, 453–461.

Bhattacharyya, S., Bershtein, S., Yan, J., Argun, T., Gilson, A.I., Trauger, S.A., Shakhnovich, E.I., 2016. Transient protein-protein interactions perturb *E. coli* metabolome and cause gene dosage toxicity. elife 5, e20309.

Chagoyen, M., Pazos, F., 2011. MBRole: enrichment analysis of metabolomic data. Bioinformatics 27, 730–731.

Coleman, S.T., Fang, T.K., Rovinsky, S.A., Turano, F.J., Moye-Rowley, W.S., 2001. Expression of a glutamate decarboxylase homologue is required for normal oxidative stress tolerance in *Saccharomyces cerevisiae*. J. Biol. Chem. 276, 244–250.

Diao, H.F., Li, X.Y., Gu, J.D., Shi, H.C., Xie, Z.M., 2004. Electron microscopic investigation of the bactericidal action of electrochemical disinfection in comparison with chlorination, ozonation and Fenton reaction. Process Biochem. 39 (11), 1421–1426.

Feehily, C., Karatzas, K.A.G., 2013. Role of glutamate metabolism in bacterial responses towards acid and other stresses. J. Appl. Microbiol. 114, 11–24.

Fotakis, C., Zervou, M., 2016. NMR metabolic fingerprinting and chemometrics driven authentication of Greek grape marc spirits. Food Chem. 196, 760–768.

Friedly, E.C., Crandall, P.G., Ricke, S., O'Bryan, C.A., Martin, E.M., Boyd, L.M., 2008. Identification of *Listeria innocua* surrogates for *Listeria monocytogenes* in hamburger patties. J. Food Sci. 73, 174–178.

Hawkins, C.L., Pattison, D.I., Davies, M.J., 2002. Reaction of protein chloramines with DNA and nucleosides: evidence for the formation of radicals, protein-DNA cross-links and DNA fragmentation. Biochem. J. 365, 605–615.

Huang, Y.W., Huang, Y.R., Hung, Y.C., Hsu, S.Y., Hwang, D.F., 2008. Application of electrolyzed water in the food industry. Food Control 19, 329–345.

Huang, D.W., Sherman, B.T., Lempicki, R.A., 2009. Bioinformatics enrichment tools: paths toward the comprehensive functional analysis of large gene lists. Nucleic Acids Res. 37, 1–13.

Ignatova, M., Prévost, H., Leguerinel, I., Guillou, S., 2010. Growth and reducing capacity of *Listeria monocytogenes* under different initial redox potential. J. Appl. Microbiol. 108, 256.

Jadhav, S., Gulati, V., Fox, E.M., Karpe, A., Beale, D.J., Sevior, D., Bhave, M., Palombo, E.A., 2015. Rapid identification and source-tracking of *Listeria monocytogenes* using MALDI-TOF mass spectrometry. Int. J. Food Microbiol. 202, 1–9.

Jeong, J., Kim, J.Y., Yoon, J., 2006. The role of reactive oxygen species in the electrochemical inactivation of microorganisms. Environ. Sci. Technol. 40 (19), 6117–6122.

Jozefczuk, S., Klie, S., Catchpole, G., Szymanski, J., Cuadros-Inostroza, A., Steinhauser, D., Willmitzer, L., 2010. Metabolomic and transcriptomic stress response of *Escherichia coli*. Mol. Syst. Biol. 6, 364.

Liao, L.B., Chen, W.M., Xiao, X.M., 2007. The generation and inactivation mechanism of oxidation-reduction potential of electrolyzed oxidizing water. J. Food Eng. 78, 1326–1332.

Liu, Q., Cedric Tan, C.S., Yang, H., Wang, S., 2017a. Treatment with low-concentration acidic electrolysed water combined with mild heat to sanitise fresh organic broccoli (*Brassica oleracea*). LWT Food Sci. Technol. 79, 594–600.

Liu, Q., Wu, J.e., Lim, Z.Y., Aggarwal, A., Yang, H., Wang, S., 2017b. Evaluation of the metabolic response of *Escherichia coli* to electrolysed water by $^{1}$H NMR spectroscopy. LWT Food Sci. Technol. 79, 428–436.

Mahmoud, B.S.M., Yamazaki, K., Miyashita, K., Kawai, Y., Shin, I.-S., Suzuki, T., 2006. Preservative effect of combined treatment with electrolyzed NaCl solutions and essential oil compounds on carp fillets during convectional air-drying. Int. J. Food Microbiol. 106 (3), 331–337.

Marcén, M., Ruiz, V., Serrano, M.J., Condón, S., Mañas, P., 2017. Oxidative stress in *E. coli* cells upon exposure to heat treatments. Int. J. Food Microbiol. 241, 198–205.

Morey, A., Bowers, J.W., Bauermeister, L.J., Singh, M., Huang, T.S., McKee, S.R., 2014. Effect of salts of organic acids on *Listeria monocytogenes*, shelf life, meat quality, and consumer acceptability of beef frankfurters. J. Food Sci. 79, 54–60.

Nightingale, Z.D., Lancha, A.H., Handelman, S.K., Dolnikowski, G.G., Busse, S.C., Dratz, E.A., Handelman, G.J., 2000. Relative reactivity of lysine and other peptide-bound amino acids to oxidation by hypochlorite. Free Radic. Biol. Med. 29, 425–433.

O'Byrne, C.P., Booth, I.R., 2002. Osmoregulation and its importance to food-borne microorganisms. Int. J. Food Microbiol. 74, 203–216.

Park, H., Hung, Y.C., Chung, D., 2004. Effects of chlorine and pH on efficacy of electrolyzed water for inactivating *Escherichia coli* O157:H7 and *Listeria monocytogenes*. Int. J. Food Microbiol. 91, 13–18.

Park, Y.B., Guo, J.Y., Rahman, S.M.E., Ahn, J., Oh, D.H., 2009. Synergistic effect of electrolyzed water and citric acid against *Bacillus cereus* cells and spores on cereal grains. J. Food Sci. 74, 185–189.

Rahman, S.M.E., Khan, I., Oh, D.H., 2016. Electrolyzed water as a novel sanitizer in the food industry: current trends and future perspectives: applications of electrolyzed water. Compr. Rev. Food Sci. Food Saf. 15, 471–490.

Silva-Angulo, A.B., Zanini, S.F., Rodrigo, D., Rosenthal, A., Martinez, A., 2014. Growth kinetics of *Listeria innocua* and *Listeria monocytogenes* under exposure to carvacrol and the occurrence of sublethal damage. Food Control 37, 336–342.

Sow, L.C., Tirtawinata, F., Yang, H., Shao, Q., Wang, S., 2017. Carvacrol nanoemulsion combined with acid electrolysed water to inactivate bacteria, yeast in vitro and native microflora on shredded cabbages. Food Control 76, 88–95.

Uyttendaele, M., Rajkovic, A., Van Houteghem, N., Boon, N., Thas, O., Debevere, J., Devlieghere, F., 2008. Multi-method approach indicates no presence of sub-lethally injured *Listeria monocytogenes* cells after mild heat treatment. Int. J. Food Microbiol. 123 (3), 262–268.

van den Berg, R.A., Hoefsloot, H.C., Westerhuis, J.A., Smilde, A.K., van der Werf, M.J.,

2006. Centering, scaling, and transformations: improving the biological information content of metabolomics data. BMC Genomics 7, 142.
Wesche, A.M., Gurtler, J.B., Marks, B.P., Ryser, E.T., 2009. Stress, sublethal injury, resuscitation, and virulence of bacterial foodborne pathogens. J. Food Prot. 72 (5), 1121–1138.
Wiklund, S., Johansson, E., Sjöström, L., Mellerowicz, E.J., Edlund, U., Shockcor, J.P., Trygg, J., 2008. Visualization of GC/TOF-MS-based metabolomics data for identification of biochemically interesting compounds using OPLS class models. Anal. Chem. 80, 115–122.
Xuan, X.T., Ding, T., Li, J., Ahn, J.H., Zhao, Y., Chen, S.G., Liu, D.H., 2017. Estimation of growth parameters of *Listeria monocytogenes* after sublethal heat and slightly acidic electrolyzed water (SAEW) treatment. Food Control 71, 17–25.
Yang, H., Feirtag, J., Diez-Gonzalez, F., 2013. Sanitizing effectiveness of commercial "active water" technologies on *Escherichia coli* O157:H7, *Salmonella enterica* and *Listeria monocytogenes*. Food Control 33, 232–238.
Ye, Y., Wang, X., Zhang, L., Lu, Z., Yan, X., 2012a. Unraveling the concentration-dependent metabolic response of *Pseudomonas* sp. HF-1 to nicotine stress by $^{1}$H NMR-based metabolomics. Ecotoxicology 21, 1314–1324.
Ye, Y., Zhang, L., Hao, F., Zhang, J., Wang, Y., Tang, H., 2012b. Global metabolomic responses of *Escherichia coli* to heat stress. J. Proteome Res. 11, 2559–2566.
Zhang, J., Yang, H., 2017. Effects of potential organic compatible sanitisers on organic and conventional fresh-cut lettuce (*Lactuca sativa* Var. *Crispa* L). Food Control 72, 20–26.
Zhang, C., Cao, W., Hung, Y.-C., Li, B., 2016. Disinfection effect of slightly acidic electrolyzed water on celery and cilantro. Food Control 69, 147–152.
Zhang, J., Zhou, S., Chen, R., Yang, H., 2017. Development of a portable electrolytic sanitising unit for the production of neutral electrolysed water. LWT Food Sci. Technol. 82, 207–215.
Zhao, L., Zhang, Y., Yang, H., 2017. Efficacy of low concentration neutralised electrolysed water and ultrasound combination for inactivating *Escherichia coli* ATCC 25922, *Pichia pastoris* GS115 and *Aureobasidium pullulans* 2012 on stainless steel coupons. Food Control 73, 889–899.